Eur. Phys. J. B **32**, 507–511 (2003)
DOI: 10.1140/epjb/e2003-00130-7

THE EUROPEAN PHYSICAL JOURNAL B

Numerical analysis of reversible A + B ↔ C reaction-diffusion systems

Z. Koza[a]

Institute of Theoretical Physics, University of Wrocław, plac Maxa Borna 9, 50204 Wrocław, Poland

Received 6 June 2002 / Received in final form 20 January 2003
Published online 7 May 2003 –

Abstract. We develop an effective numerical method of studying large-time properties of reversible reaction-diffusion systems of type A + B ↔ C with initially separated reactants. Using it we find that there are three types of asymptotic reaction zones. In particular we show that the reaction rate can be locally negative and concentrations of species A and B can be nonmonotonic functions of the space coordinate x, locally significantly exceeding their initial values.

PACS. 66.30.Ny Chemical interdiffusion; diffusion barriers – 82.20.-w Chemical kinetics and dynamics – 02.60.Lj Ordinary and partial differential equations; boundary value problems

1 Introduction

Dynamic reaction fronts formed between initially separated reactants A and B that perform Brownian motion and react upon contact are an important component of many physical, chemical and biological systems [1,2]. Most theoretical [3–14], numerical [15] and experimental [16–20] research has been focused on *irreversible* reactions of type A + B → C, which exhibit many unexpected phenomena. For example, the width of the reaction zone grows with time t as t^α with surprisingly small value of $\alpha = 1/6$ [3,4], the center of the reaction front can spontaneously change the direction of its motion [8,17], and the mean-field approximation of the local reaction rate breaks down at and below the critical dimension $d_c = 2$ [6,7,15].

In reality, however, most chemical reactions are reversible. The simplest model of such a system [21] is based on an assumption that concentrations a, b, and c of species A, B, and C, respectively, effectively depend on time t and only one space coordinate x (even though the system is three-dimensional), and their evolution is governed by three reaction-diffusion equations

$$\frac{\partial a(x,t)}{\partial t} = D_A \frac{\partial^2 a(x,t)}{\partial x^2} - R(x,t), \tag{1}$$

$$\frac{\partial b(x,t)}{\partial t} = D_B \frac{\partial^2 b(x,t)}{\partial x^2} - R(x,t), \tag{2}$$

$$\frac{\partial c(x,t)}{\partial t} = D_C \frac{\partial^2 c(x,t)}{\partial x^2} + R(x,t), \tag{3}$$

where the effective local reaction rate $R(x,t)$ equals to the difference between the production (A + B $\xrightarrow{k}$ C) and decay (C $\xrightarrow{g}$ A + B) rates of species C,

$$R(x,t) \equiv ka(x,t)b(x,t) - gc(x,t). \tag{4}$$

Here D_A, D_B, and D_C are diffusion coefficients of species A, B, and C, respectively, and $k, g > 0$ are reaction rate constants. It is also assumed that initially species A and B are uniformly distributed on opposite sides of $x = 0$ with concentrations a_0 and b_0, respectively,

$$a(x,0) = a_0 H(x), \quad b(x,0) = b_0 H(-x), \quad c(x,0) = 0, \tag{5}$$

where $H(x)$ is the Heaviside step function (which is 0 for $x < 0$ and 1 for $x > 0$). Such an initial condition is often adopted in experiments [16–20] and simplifies theoretical analysis, as it enables reduction of a three-dimensional problem to a one-dimensional one.

This model was first studied by Chopard *et al.* [21]. They found that (a) the front width of a reversible reaction asymptotically scales with time as if the process was governed solely by diffusion ($w(t) \propto t^{1/2}$) and (b) the mean-field approximation (4) can be safely applied for systems of spatial dimension $d = 1, 2, 3$. However, the fundamental problem of giving a detailed description of spatiotemporal evolution of reversible reaction-diffusion systems remained open until quite recently.

This problem was recently considered by Sinder and Pelleg [11–13]. They focused their attention mainly on the limit of a vanishingly small backward reaction rate g and found that in this limit concentrations of species A, B, and C assume the forms typical of irreversible reactions ($g = 0$) everywhere except in a very narrow reaction zone. They confirmed the result of reference [21] that there is

[a] e-mail: zkoza@ift.uni.wroc.pl

a crossover between intermediate-time "irreversible" and large-time "reversible" regimes. They showed that the asymptotic reaction rate R can have one or two maxima and can even be locally negative (for irreversible reactions R always has a single maximum an can never be negative). Moreover, they presented strong arguments supporting a conjecture that reversible reaction-diffusion processes can be divided into two distinct universality classes. One of them contains systems with immobile reaction product C and asymptotically immobile reaction front, while systems with all other combination of the control parameters form the other universality class.

In our recent paper [22] we developed a new approach, enabling one to analyze the large-time limit of reversible reaction-diffusion systems *directly*, without having to solve the original partial differential equations (1–3) and then taking the limit $t \to \infty$. We proved that in the large-time limit functions $a(x,t)$, $b(x,t)$, $c(x,t)$, and $R(x,t)$ effectively depend on x only through $\xi \equiv x/\sqrt{t}$ and take on a form

$$a(x,t) = \mathcal{A}(\xi), \quad b(x,t) = \mathcal{B}(\xi), \quad c(x,t) = \mathcal{C}(\xi),$$
$$R(x,t) = t^{-1}\mathcal{R}_1(\xi) \tag{6}$$

where the scaling functions $\mathcal{A}$, $\mathcal{B}$, $\mathcal{C}$, and $\mathcal{R}_1$ are completely determined by four equations

$$k\mathcal{A}\mathcal{B} - g\mathcal{C} = 0, \tag{7}$$

$$D_A\frac{\mathrm{d}^2\mathcal{A}}{\mathrm{d}\xi^2} + \frac{1}{2}\xi\frac{\mathrm{d}\mathcal{A}}{\mathrm{d}\xi} = \mathcal{R}_1 \tag{8}$$

$$D_B\frac{\mathrm{d}^2\mathcal{B}}{\partial\xi^2} + \frac{1}{2}\xi\frac{\mathrm{d}\mathcal{B}}{\mathrm{d}\xi} = \mathcal{R}_1 \tag{9}$$

$$D_C\frac{\mathrm{d}^2\mathcal{C}}{\mathrm{d}\xi^2} + \frac{1}{2}\xi\frac{\mathrm{d}\mathcal{C}}{\mathrm{d}\xi} = -\mathcal{R}_1 \tag{10}$$

with the boundary conditions

$$\lim_{\xi\to-\infty}\mathcal{A}(\xi) = a_0, \quad \lim_{\xi\to\infty}\mathcal{A}(\xi) = 0, \tag{11}$$
$$\lim_{\xi\to-\infty}\mathcal{B}(\xi) = 0, \quad \lim_{\xi\to\infty}\mathcal{B}(\xi) = b_0. \tag{12}$$

Compared with the original problem of solving equations (1–3), this new approach has two advantages. First, it involves only ordinary differential equations. Second, it pertains directly to the large-time limit.

In principle equations (7–10) completely determine the asymptotic, large-time spatiotemporal evolution of an arbitrary reversible reaction-diffusion system. Unfortunately, they are quite complex and a complete analytical solution is known only for the case $D_A = D_B = D_C$ [22]. The aim of our paper is to examine these equations numerically for other values of the control parameters.

2 Numerical results

By measuring length, time, and concentration in units of $\sqrt{D_A/ka_0}$, $1/ka_0$, and a_0, respectively, the general problem of solving (5–10) for arbitrary values of a_0, b_0, D_A, D_B, D_C, k, and g can be reduced to the one with [21]

$$D_A = 1, \quad a_0 = 1, \quad k = 1. \tag{13}$$

We shall adopt these particular values in our further analysis. This will leave us with four independent control parameters: g, b_0, D_B, and D_C.

Our basic equations (7–10) can be reduced to two ordinary differential equations with two unknown functions $\mathcal{A}(\xi)$ and $\mathcal{B}(\xi)$,

$$\frac{\mathrm{d}^2\left(\mathcal{A} + D_C g^{-1}\mathcal{A}\mathcal{B}\right)}{\mathrm{d}\xi^2} = -\frac{1}{2}\xi\frac{\mathrm{d}\left(\mathcal{A} + g^{-1}\mathcal{A}\mathcal{B}\right)}{\mathrm{d}\xi} \tag{14}$$

$$\frac{\mathrm{d}^2\left(D_B\mathcal{B} + D_C g^{-1}\mathcal{A}\mathcal{B}\right)}{\mathrm{d}\xi^2} = -\frac{1}{2}\xi\frac{\mathrm{d}\left(\mathcal{B} + g^{-1}\mathcal{A}\mathcal{B}\right)}{\mathrm{d}\xi}. \tag{15}$$

To solve them we employed an iterative method. We first assumed that $\mathcal{B}_0(\xi) = 0$ and, using standard techniques [23], solved (14) as a *linear* ordinary differential equation for $\mathcal{A}_0(\xi)$ with boundary condition (11). We inserted this solution into (15), which was then solved as a linear differential equation for $\mathcal{B}_0(\xi)$. This solution was again inserted into (14) and used to determine the next approximation of $\mathcal{A}_0(\xi)$. This procedure was repeated until a required accuracy was achieved.

Taking $\mathcal{B}_0(\xi) = 0$ as the first approximation leads to exact solution for $g^{-1} = 0$ (or, equivalently, $k = 0$) after the first iteration cycle, and ensures quick convergence for most choices of system parameters except when $g \ll 1$. In this case the reaction zone is very narrow and inside it functions $\mathcal{A}_0(\xi)$ and $\mathcal{B}_0(\xi)$ vary very rapidly, which makes the direct iterative method unstable. This problem may be circumvented by first solving (14) and (15) for $g \sim 1$ and then decreasing g gradually until it reaches the required value, each time employing a solution obtained for larger g as an initial guess for a smaller value of g. Once $\mathcal{A}(\xi)$ and $\mathcal{B}(\xi)$ have been determined, the two remaining functions of primary interest, $\mathcal{C}(\xi)$ and $\mathcal{R}_1(\xi)$ can be calculated directly from (7) and (8), respectively.

The iterative method cannot be applied directly for $D_B = D_C = 0$, as in this case the left-hand side of (15) vanishes and the order of this differential equation equals 1 rather than 2. Nevertheless, since in this very particular case $b(x,t) + c(x,t) = b_0 H(x)$, after some simple algebra we can reduce (14) and (15) to a single equation

$$\frac{\mathrm{d}^2\mathcal{A}(\xi)}{\mathrm{d}\xi^2} = -\frac{1}{2}\xi\frac{\mathrm{d}\mathcal{A}(\xi)}{\mathrm{d}\xi}\left(1 + \frac{b_0 H(\xi)}{\left[g + \mathcal{A}(\xi)\right]^2}\right). \tag{16}$$

Although this equation looks very complicated, it can be solved quite easily through standard numerical methods.

To estimate accuracy of the iterative method, we used it to solve equations (14) and (15) for the case of equal diffusion constants, $D_A = D_B = D_C = 1$, and compared the results with the exact solutions obtained in reference [22]. For $b_0 = 1$, 0.1, 0.01, $g = 100$, 1, 0.01, and $-5 < \xi < 5$ we found the relative error to be less than 10^{-6}.

Next we used (14–16) to investigate thoroughly various combinations of system parameters. To ensure that

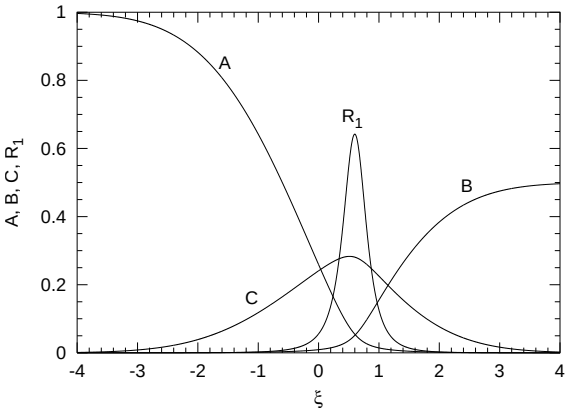

Fig. 1. $\mathcal{A}$, $\mathcal{B}$, $\mathcal{C}$, and $\mathcal{R}_1$ (asymptotic concentrations of species A, B, C, and the scaling function of the reaction rate, respectively), as functions of $\xi \equiv x/\sqrt{t}$ for $a_0 = 1$, $b_0 = 0.5$, $D_A = D_B = D_C = 1$, $k = 1$ and $g = 0.01$. Arbitrary units.

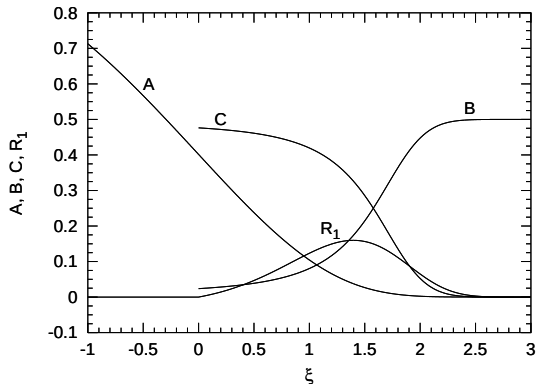

Fig. 2. $\mathcal{A}$, $\mathcal{B}$, $\mathcal{C}$, and $\mathcal{R}_1$ as functions of $\xi \equiv x/\sqrt{t}$ for $a_0 = 1$, $b_0 = 0.5$, $D_A = 1$, $D_B = D_C = 0$, $k = 1$ and $g = 0.02$. Note that $\mathcal{B}(\xi)$ and $\mathcal{C}(\xi)$ vanish for $\xi < 0$. Arbitrary units.

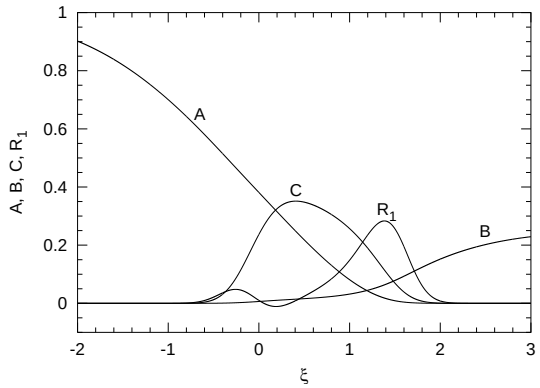

Fig. 3. $\mathcal{A}$, $\mathcal{B}$, $\mathcal{C}$, and $\mathcal{R}_1$ as functions of $\xi \equiv x/\sqrt{t}$ for $a_0 = 1$, $b_0 = 0.25$, $D_A = D_B = 1$, $D_C = 0.01$, $k = 1$ and $g = 0.01$. Note that $\mathcal{R}_1(\xi)$ can assume negative values. Arbitrary units.

the boundary conditions (11–12) are actually satisfied, we used a rather wide range $-10 \le \xi \le 10$ and compared the results thus obtained with those calculated for $-15 \le \xi \le 15$, finding no significant differences. Moreover, upon a thorough numerical scanning of the four-dimensional parameter space we found that the solutions of equations (7–10) are continuous functions of D_B, D_C, g, and b_0 (even when going from one of Sinder and Pelleg's universality classes to the other), and can be divided into three major categories distinguished by specific forms of the local reaction rate $\mathcal{R}_1$.

2.1 Reaction fronts of type I

A characteristic feature of reaction fronts of type I is that the asymptotic reaction rate $\mathcal{R}_1(\xi)$ is positive for all ξ and has a single maximum, which may be identified with the reaction front center ξ_f. A typical example of such a reaction front is illustrated in Figure 1, which was obtained for $b_0 = 0.5$, $D_A = D_B = D_C = 1$, and $g = 0.01$. As in this case $\xi_f > 0$, we may say that the reaction front moves towards the right-hand side of the system. This type of solution always appears for $D_A = D_B = D_C$ [22] and for $g = 0$ [3], and so we expect it also to appear for $D_A \approx D_B \approx D_C$ or for $g \ll 1$.

Interestingly, it turns out that the reaction front formed in the case $D_B = D_C = 0$ also belongs to this category. This is clearly seen in Figure 2, obtained for $D_B = D_C = 0$, $b_0 = 0.5$, and $g = 0.02$. A characteristic feature of this case is discontinuity of $\mathcal{B}(\xi)$ and $\mathcal{C}(\xi)$ at $\xi = 0$. This reflects the presence of the Heaviside function in equation (16).

2.2 Reaction fronts of type II

An example of the second type of the asymptotic solution is depicted in Figure 3, which was obtained for much smaller value of $D_C = 0.01$ (the values of other control parameters were $D_B = 0.5$, $b_0 = 0.25$, and $g = 0.01$). In this case $\mathcal{R}_1$ has two maxima $\xi_1^{\max} \approx -0.26$ and $\xi_2^{\max} \approx 1.38$. As they are of opposite signs, the system apparently has two reaction fronts moving at opposite directions. Moreover, the reaction rate has one minimum, $\xi^{\min} \approx 0.19$, at which it attains a negative value. In the region where $\mathcal{R}_1 < 0$ the backward reaction ($\mathrm{C} \xrightarrow{g} \mathrm{A} + \mathrm{B}$) is thus locally faster than the forward reaction ($\mathrm{A} + \mathrm{B} \xrightarrow{k} \mathrm{C}$), although of course the global reaction rate $\int_0^\infty \mathcal{R}_1(\xi)\,\mathrm{d}\xi > 0$.

Formation of a region with negative value of $\mathcal{R}_1$ can be understood as follows. Consider an asymmetric reaction-diffusion system with very small diffusion coefficient of species C ($D_C \ll D_A, D_B$) and a small backward reaction rate g. As the reaction proceeds, the reaction front moves through the system, leaving behind a region filled with practically immobile and very slowly decaying reaction product C. At some moment the mobile reaction front will leave this region, and so the backward reaction, however small, may start to dominate. This may lead to formation of a region where $\mathcal{R}_1(\xi)$ attains a locally minimal, perhaps even negative value.

The dominant backward reaction should lead to production of additional molecules of type A and B. Because $D_A, D_B \gg D_C$, these molecules can easily diffuse away

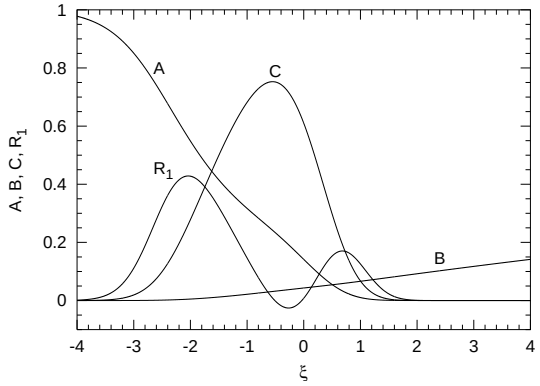

Fig. 4. $\mathcal{A}$, $\mathcal{B}$, $\mathcal{C}$, and $\mathcal{R}_1$ as functions of $\xi \equiv x/\sqrt{t}$ for $a_0 = 1$, $b_0 = 0.25$, $D_A = 1$, $D_B = 32$, $D_C = 0.01$, $k = 1$ and $g = 0.01$. Arbitrary units.

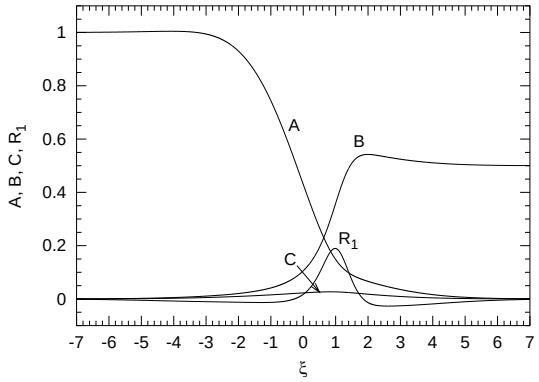

Fig. 5. $\mathcal{A}$, $\mathcal{B}$, $\mathcal{C}$, and $\mathcal{R}_1$ as functions of $\xi \equiv x/\sqrt{t}$ for $a_0 = 1$, $b_0 = 0.5$, $D_A = 1$, $D_B = 0.1$, $D_C = 10$, $k = 1$ and $g = 2$. Note that $\mathcal{A}_0(\xi)$ and $\mathcal{B}_0(\xi)$ are nonmonotonic and $\mathcal{R}_1$ can be negative. Arbitrary units.

from the region filled with molecules C. Then, at the other edge of the region rich in species C, they should give a significant contribution to the forward reaction rate, forcing $\mathcal{R}_1(\xi)$ to change its sign back to positive and forming the other reaction front. Such scenario is confirmed by Figure 3, which shows that molecules B are present in the whole region densely occupied by molecules C, including a region between $\xi_1^{\max}$ and 0. Molecules of type B are present in this region even though the main reaction front, located near $\xi_2^{\max}$, is constantly moving away.

Reaction fronts of type II were first observed by Sinder and Pelleg [13] in systems with $D_C = 0$. They came to the conclusion that for mobile reaction fronts ($x_f(t) \neq 0$) the larger maximum is located near the point where $a(x,t) \approx b(x,t)$. However, we found that the opposite situation is also possible. This is illustrated in Figure 4, obtained for $D_C = 0.01$, $D_B = 32$, $b_0 = 0.25$, and $g = 0.01$. As we can see, in this case $a(x) \approx b(x)$ near the second, much smaller maximum of $R_1(x)$.

We expect reaction fronts of type II to be typical of systems where either D_B or D_C are much smaller than D_A. We base this conjecture on equations (9, 10) which ensure that if $D_C = 0$ or $D_B = 0$ then $R_1(0) = 0$. Since $R_1(\xi)$ is continuous we may thus expect that at least for highly asymmetric reaction fronts $R_1(\xi)$ will attain negative values in the vicinity of $\xi = 0$.

2.3 Reaction fronts of type III

It turns out that $\mathcal{A}_0(\xi)$ and $\mathcal{B}_0(\xi)$ may be nonmonotonic functions of ξ. In this case, which we call reaction front of type III, $\mathcal{R}_1(\xi)$ has a single maximum surrounded by two minimums at which $\mathcal{R}_1(\xi) < 0$. All these properties are clearly seen in Figure 5, obtained for $D_C = 10$, $D_B = 0.1$, $b_0 = 0.5$, and $g = 2$.

This type of a reaction front can be uniquely identified by determining whether the maximal value of a, denoted $a_{\max}$, exceeds a_0 (or, similarly, whether $b_{\max} > b_0$). We employed this criterion in our numerical calculations. On extensive scanning of the 4-dimensional space of free parameters we came to the conclusion that the necessary

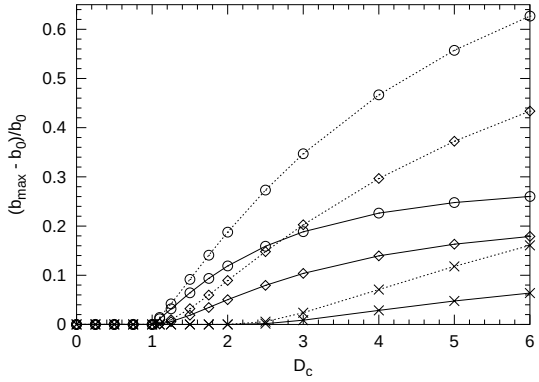

Fig. 6. The maximal relative increase of the concentration of species B, $\tilde{\Delta} b_{\max} \equiv (b_{\max} - b_0)/b_0$, as a function of D_C for $g = 0.01$, $b_0 = 0.01$ (solid lines), 0.001 (dashed lines), $D_B = 0$ ($\circ$), 0.5 ($\diamond$), and 2 ($\times$). Arbitrary units.

and sufficient condition for this type of the asymptotic reaction front reads

$$D_C > \max(D_A, D_B). \tag{17}$$

However, only for $D_C \gg \max(D_A, D_B)$ is the effect really significant. We also found that the maximal relative increase in concentrations of species B, $\tilde{\Delta} b_{\max} \equiv (b_{\max} - b_0)/b_0$, is an increasing function of D_C and a decreasing function of both b_0 and D_B. In particular $\tilde{\Delta} b_{\max}$ turns out to be very sensitive to changes of b_0, *i.e.* a parameter that can be easily controlled experimentally. As for g, $\tilde{\Delta} b_{\max}$ attains a maximal value at $g \approx 1$ and decreases as $g \to 0$ or $g \to \infty$. These findings are depicted in Figure 6, which presents $\tilde{\Delta} b_{\max}$ as a function of D_C obtained for $g = 0.01$, $b_0 = 0.01$ (solid lines), 0.001 (dashed lines), and $D_B = 0$ (circles), 0.5 (diamonds), 2.0 (crosses). As we can see, $\tilde{\Delta} b_{\max}$ can attain quite high values, exceeding 60%.

The unusual features of this asymptotic solution can be explained as follows. For $D_C \gg D_A, D_B$ molecules C quickly diffuse away from the reaction layer. They may

thus form a region where the reverse reaction dominates the forward one, leading to $\mathcal{R}_1(\xi) < 0$. The same phenomenon brings about production of additional backward reaction products A and B outside the main reaction zone. For suitably chosen system parameters this can result in a situation where $\mathcal{A}_0(\xi)$ and $\mathcal{B}_0(\xi)$ are nonmonotonic. This effect should become more pronounced with increased velocity of the reaction zone (*i.e.*, when b_0, $D_B \to 0$) and becomes negligibly small as $g \to 0$ (negligible backward reaction) or $g \to \infty$ (negligible forward reaction).

3 Conclusions

We have analyzed numerically the large-time properties of reaction fronts formed in reversible reaction-diffusion systems of type A + B ↔ C. We found that, depending on the values of control parameters, reversible reaction fronts can be divided into three categories. In reaction fronts of type I the local reaction rate is always positive and has a well defined, single maximum. In reaction fronts of type II the local reaction rate has two maxima, moving in opposite directions, and a single minimum, which can attain a negative value. In reaction fronts of type III the local reaction rate has a single maximum surrounded by two minima, at which it attains negative values; moreover, the concentrations of species A and B are here locally larger than their initial values. Our numerical calculations indicate that the condition for this type of reaction front is given by a formula $D_C > \max(D_A, D_B)$ and that the effect of the local increase in concentration of species A or B can be easily controlled experimentally through their initial concentrations a_0 or b_0.

We found that the large-time behaviour of reversible reaction-diffusion systems is richer than that of irreversible ones. Depending on the values of the control parameters one can expect qualitatively different asymptotic solutions. Although the "anomalous" effects are rather small, we believe that they could be observed experimentally. It would be particularly interesting to investigate effects of nonmonotonic dependence of concentrations of reactants A and B on the space coordinate x in systems with reaction fronts of type III. If the A + B ↔ C reaction were a part of a more complex reaction scheme such that additional reaction steps (*e.g.* precipitation) could occur only above some threshold values of the reactant concentrations (*e.g.* nucleation thresholds), setting a_0 or b_0 just below such a threshold value might lead to some interesting phenomena. An example of such a complex process is formation of the Liesegang patterns, which are quasiperiodic precipitation patterns emerging in the wake of a mobile chemical reaction front [24,25]. Our study indicates that it should be possible to obtain similar precipitation patterns of species B in reaction-diffusion systems with reversible reaction of type A + B ↔ C, diffusion coefficients $D_C \gg D_A, D_B$, and initial concentrations $a_0 \gg b_0$.

References

1. S.A. Rice, *Diffusion Limited Reactions* (Elsevier, Amsterdam, 1985)
2. D. ben Avraham, S. Havlin, *Diffusion and Reactions in Fractals and Disordered Systems* (Cambridge Univ. Press, Cambridge, 2000)
3. L. Galfi, Z. Rácz, Phys. Rev. A **38**, 3151 (1988)
4. A. Schenkel, P. Wittwer, J. Stubbe, Physica D **69**, 135 (1993)
5. H. Taitelbaum, S. Havlin, J.E. Kiefer, B. Trus, G.H. Weiss, J. Stat. Phys. **65**, 873 (1991)
6. S. Cornell, M. Droz, Phys. Rev. Lett. **70**, 3824 (1993)
7. B.P. Lee, J. Cardy, Phys. Rev. E **50**, R3287 (1994)
8. Z. Koza, H. Taitelbaum, Phys. Rev. E **54**, R1040 (1996)
9. Z. Koza, J. Stat. Phys. **85**, 179 (1996)
10. Z. Koza, Physica A **240**, 622 (1997)
11. M. Sinder, J. Pelleg, Phys. Rev. E **60**, R6259 (1999)
12. M. Sinder, J. Pelleg, Phys. Rev. E **61**, 4935 (2000)
13. M. Sinder, J. Pelleg, Phys. Rev. E **62**, 3340 (2000)
14. J. Magnin, Eur. Phys. J. B **17**, 673 (2000)
15. S. Cornell, Phys. Rev. E **51**, 4055 (1995)
16. Y.-E.L. Koo, R. Kopelman, J. Stat. Phys. **65**, 893 (1991)
17. H. Taitelbaum, Y.-E.L. Koo, S. Havlin, R. Kopelman, G.H. Weiss, Phys. Rev. A **46**, 2151 (1992)
18. A. Yen, Y. Koo, R. Kopelman, Phys. Rev. E **54**, 2447 (1996)
19. S.H. Park, S. Parus, R. Kopelman, H. Taitelbaum, Phys. Rev. E **64**, 055102(R) (2001)
20. C. Leger, F. Argoul, M.Z. Bazant, J. Phys. Chem. B **103**, 5841 (1999)
21. B. Chopard, M. Droz, T. Karapiperis, Z. Rácz, Phys. Rev. E **47**, R40 (1993)
22. Z. Koza, Phys. Rev. E **66**, 011103 (2002)
23. W.H. Press, S.A. Teukolsky, W.T. Vetterling, B.P. Flannery, *Numerical Recipies in C* (Cambridge Univ. Press, Cambridge, 1992)
24. B. Chopard, P. Luthi, M. Droz, Phys. Rev. Lett. **72**, 1384 (1994)
25. T. Antal, M. Droz, J. Magnin, A. Pękalski, J. Chem. Phys. **114**, 3770 (2001)